Cell, Vol. 84, 745–755, March 8, 1996, Copyright ©1996 by Cell Press

Inactivation of NMDA Receptors by Direct Interaction of Calmodulin with the NR1 Subunit

Michael D. Ehlers,*† Su Zhang,*† Jeffrey P. Bernhardt,* Richard L. Huganir*
*Department of Neuroscience
Howard Hughes Medical Institute
The Johns Hopkins University School of Medicine
Baltimore, Maryland 21205

Summary

NMDA (N-methyl-D-aspartate) receptors are excitatory neurotransmitter receptors in the brain critical for synaptic plasticity and neuronal development. These receptors are Ca^{2+}-permeable glutamate-gated ion channels whose physiological properties are regulated by intracellular Ca^{2+}. We report here the purification of a 20 kDa protein identified as calmodulin that interacts with the NR1 subunit of the NMDA receptor. Calmodulin binding to the NR1 subunit is Ca^{2+} dependent and occurs with homomeric NR1 complexes, heteromeric NR1/NR2 subunit complexes, and NMDA receptors from brain. Furthermore, calmodulin binding to NR1 causes a 4-fold reduction in NMDA channel open probability. These results demonstrate that NMDA receptor function can be regulated by direct binding of calmodulin to the NR1 subunit, and suggest a possible mechanism for activity-dependent feedback inhibition and Ca^{2+}-dependent inactivation of NMDA receptors.

Introduction

NMDA (N-methyl-D-aspartate) receptors constitute a major class of glutamate-gated ion channels in the central nervous system (for reviews, see Seeburg, 1993; Wisden and Seeburg, 1993; Hollmann and Heinemann, 1994). NMDA receptors are found in almost all central nervous system neurons (Petralia et al., 1994), where they play an important role in synaptogenesis, synaptic plasticity, and excitotoxicity (Constantine-Paton et al., 1990; Bliss and Collingridge, 1993; Choi, 1995). In contrast to most other glutamate receptors, NMDA receptor channels exhibit high permeability to Ca^{2+} and voltage-dependent block by Mg^{2+} (Mayer et al., 1984; MacDermott et al., 1986). This Ca^{2+} permeability and Mg^{2+} block underlie NMDA receptor-dependent plasticity in the nervous system (Bliss and Collingridge, 1993). NMDA receptors are oligomeric complexes comprised of members of two families of homologous subunits, NR1 and NR2A–D (Moriyoshi et al., 1991; Kutsuwada et al., 1992; Meguro et al., 1992; Monyer et al., 1992). Additional molecular diversity of NMDA receptors arises through alternative splicing of NR1 mRNA. At least seven NR1 splice variants (NR1a–NR1g) are expressed in the central nervous system (Durand et al., 1992; Sugihara et al., 1992; Hollmann et al., 1993), arising through the insertion or deletion of three short exon cassettes in the NH_2-terminal (N1), and COOH-terminal (C1, C2) regions of the NR1 molecule. These NR1 splice variants differ in their spatial and temporal expression patterns (Laurie and Seeburg, 1994), their sensitivity to phorbol esters, polyamines, protons, and Zn^{2+} (Durand et al., 1992; Hollmann et al., 1993; Traynelis et al., 1995), their ability to be phosphorylated by protein kinase C (Tingley et al., 1993), and their subcellular localization in heterologous expression systems (Ehlers et al., 1995).

NMDA receptors are regulated by a wide array of extracellular agents, including Mg^{2+}, glycine, Zn^{2+}, and protons, (Collingridge and Lester, 1989; Hollman and Heinemann, 1994), as well as intracellular signals including protein kinases and protein phosphatases (Lieberman and Mody, 1994; Roche et al., 1994; Tong et al., 1995). In addition, numerous studies have shown that intracellular Ca^{2+} can transiently inhibit the activity of NMDA receptor channels (Mayer and Westbrook, 1985; Zorumski et al., 1989; Legendre et al., 1993; Vyklicky, 1993; Medina et al., 1995). This Ca^{2+}-dependent NMDA receptor inactivation is unaffected by ATP, many types of phosphatase inhibitors, and other agents that affect protein phosphorylation (Legendre et al., 1993; Rosenmund and Westbrook, 1993a; Vyklicky, 1993), although recent studies have shown that NMDA receptors are inactivated by the Ca^{2+}-calmodulin-dependent protein phosphatase calcineurin (Lieberman and Mody, 1994; Tong et al., 1995). Further studies have indicated that Ca^{2+}-dependent desensitization might be mediated by linkage of the NMDA receptor to the actin cytoskeleton in a manner regulated by a Ca^{2+}-sensitive protein (Rosenmund and Westbrook, 1993b). This Ca^{2+}-dependent inactivation of NMDA receptors provides a feedback mechanism capable of regulating subsequent Ca^{2+} entry into the postsynaptic cell through NMDA channels.

This study demonstrates that calmodulin (CaM) binds directly to the NR1 subunit of the NMDA receptor complex in a Ca^{2+}-dependent manner. The binding of CaM to the NR1 subunit is shown to occur at two distinct sites in the COOH-terminal region of the molecule, which have different affinities for CaM. One of the CaM binding sites is wholly contained within the alternatively spliced C1 exon cassette, whereas the other is found in a region common to all NR1 splice variants. CaM binding to these sites is further shown to reduce both the open rate and mean open time of NMDA receptor channels isolated in excised patches. Our results identify CaM as an intracellular signaling molecule capable of directly binding to and regulating NMDA receptor function.

Results

Identification of CaM as an NR1 Binding Protein

Previous studies have demonstrated both differential subcellular distribution in transfected cells (Ehlers et al., 1995) and differential phosphorylation (Tingley et al., 1993) of NR1 subunit splice variants containing the C1 exon cassette. To further examine the role of the C1

† These authors contributed equally to this work.

cassette in NMDA receptor function, proteins that specifically associate with C1 cassette–containing NR1 splice variants were identified by coimmunoprecipitation studies. QT6 quail fibroblasts were mock transfected or transfected with the cDNAs encoding either the NR1a (C1+) or NR1c (C1−) splice variants, and the cells metabolically labeled using ^{35}S-methionine and ^{35}S-cysteine. The QT6 quail fibroblast line has been previously used as a model system for studying nicotinic acetylcholine receptor clustering (Phillips et al., 1991), as well as NR1 splice variant subcellular distribution (Ehlers et al., 1995). Immunoprecipitation of NR1 subunits along with associated proteins revealed the presence of a prominent 20 kDa protein that preferentially coprecipitated with the NR1a subunit (Figure 1A). A protein of similar molecular weight from metabolically labeled QT6 cells also bound to an NR1 COOH-terminus fusion protein affinity resin (Figures 1B and 1C). Interestingly, at 150 mM NaCl with 1% NP-40, this protein bound to both the NR1a and NR1c COOH-terminal fusion proteins, but not hexahistidine backbone fusion protein (Figure 1B, left). When the NaCl concentration was increased to 500 mM, however, the prominent 20 kDa protein preferentially associated with the NR1a COOH-terminal fusion protein (Figure 1B, middle). With more stringent detergent conditions (RIPA buffer: 1% NP-40, 0.5% deoxycholate, 0.1% SDS), binding of the 20 kDa protein to both NR1 COOH-terminal fusion proteins was abolished (Figure 1B, right).

To determine the identity of the 20 kDa protein, the NR1a COOH-terminus fusion protein affinity resin was used to purify ~2 μg of the protein from QT6 cell lysates for microsequencing. The sequences of four peptides were obtained (Figure 1D). Each of these four peptides was identical to an amino acid sequence contained in CaM (Figure 1D).

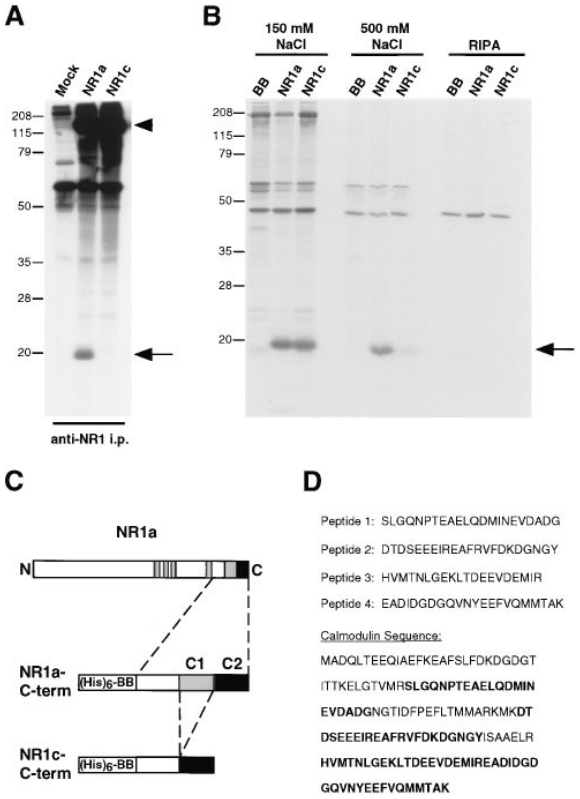

Figure 1. Purification of a 20 kDa Protein Identified as Calmodulin that Preferentially Associates with C1 Cassette–Containing NR1 Splice Variants

(A) ^{35}S-labeled QT6 cells expressing NR1a, NR1c, or mock transfected were solubilized, and complexes of the NR1 subunit along with associated proteins were coimmunoprecipitated using a polyclonal anti-NR1 antibody. Precipitated proteins were eluted, resolved by SDS-PAGE, and visualized by fluorography. The arrow indicates the prominent 20 kDa protein and the arrowhead shows NR1. Molecular mass markers in kilodaltons are shown.

(B) ^{35}S-labeled QT6 cells were solubilized using 150 mM NaCl (buffer B), 500 mM NaCl (buffer A), or RIPA buffer, and incubated with either hexahistidine backbone (BB), NR1a COOH-terminal, or NR1c COOH-terminal fusion protein affinity resin (see Experimental Procedures). Bound proteins were analyzed as in (A). The arrow indicates the bound 20 kDa protein. Molecular weight markers in kilodaltons are shown.

(C) Diagram of the NR1a subunit showing the alternatively spliced exon cassettes, C1 and C2, and the structures of the hexahistidine-tagged NR1a and NR1c COOH-terminal fusion proteins. The four originally proposed transmembrane domains are shown as narrow boxes.

(D) Comparison of the primary sequence of CaM to the sequences of four peptides (in bold) isolated by high performance liquid chromatography following proteolysis of the 20 kDa protein.

CaM Binding to NR1 Is Regulated by Both the C1 Cassette and Ca^{2+}

To verify that CaM could directly interact with the COOH-terminus of NR1, CaM was incubated with the fusion protein affinity resins. Immunoblot analysis of bound proteins using an anti-CaM antibody indicated that CaM readily binds to the COOH-terminus of NR1a in 500 mM NaCl (Figure 2A). This binding was completely abolished by removal of Ca^{2+} and addition of 5 mM EGTA, and CaM did not bind to the hexahistidine backbone fusion protein (Figure 2A). In addition, CaM was observed to bind somewhat less efficiently to the NR1c COOH-terminus in a similarly Ca^{2+}-dependent manner (Figure 2A). Coimmunoprecipitation experiments performed on lysates of QT6 cells expressing either NR1a or NR1c subunits using an anti-NR1 antibody showed that CaM coprecipitates with NR1a but not NR1c subunits, and that this coprecipitation is dependent on Ca^{2+} (Figure 2B). No CaM was observed to coprecipitate from mock transfected cell lysates. CaM also coimmunoprecipitated with the C1+ NR1d subunit, but not with the C1− NR1e subunit (data not shown). These results were consistent with those obtained using ^{35}S-labeled QT6 cell lysates (Figures 1A and 1B), and indicated that CaM could directly interact with the COOH-terminus of NR1 in a Ca^{2+}-dependent manner regulated by the presence of the C1 exon cassette.

CaM Associates with Heteromeric NR1/NR2 Complexes and with NMDA Receptors in Rat Brain

Most NMDA receptors in the brain are thought to be heteromeric complexes composed of both NR1 and NR2 subunits (Sheng et al., 1994). To determine whether CaM was capable of interacting with heteromeric NMDA receptor complexes, coimmunoprecipitation experiments

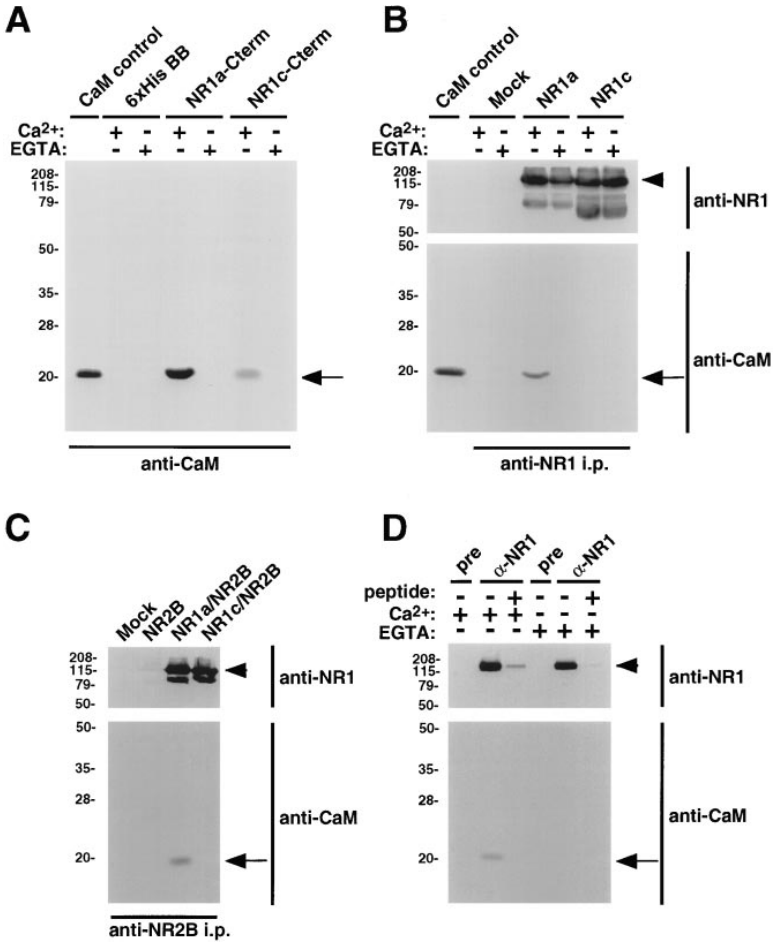

Figure 2. CaM Interacts with COOH-Terminal NR1 Fusion Proteins, Heterologously Expressed NR1 Subunits, and NR1 Subunits in the Brain

(A) Hexahistidine backbone (BB), NR1a COOH-terminal, or NR1c COOH-terminal fusion protein affinity resins were incubated with 1 μg CaM in the presence or absence of Ca^{2+} as indicated. Bound CaM was detected by immunoblot analysis using an anti-CaM monoclonal antibody. CaM (100 ng) was run as a control (CaM control).

(B) Either mock transfected, NR1a-transfected, or NR1c-transfected QT6 cells were solubilized in the presence or absence of Ca^{2+} as indicated. Complexes of NR1 subunit along with associated proteins were coimmunoprecipitated using a polyclonal anti-NR1 antibody and detected by immunoblot analysis using anti-NR1 or anti-CaM monoclonal antibodies. CaM (100 ng) was run as a control (CaM control).

(C) Coimmunoprecipitations were performed on cell lysates from QT6 cells expressing either NR2B, NR1a and NR2B, NR1c and NR2B, or mock-transfected QT6 cells using an anti-NR2B antibody followed by immunoblot analysis with anti-NR1 or anti-CaM monoclonal antibodies.

(D) Solubilized proteins from adult rat cortex were immunoprecipitated with either preimmune serum, anti-NR1 polyclonal antibody, or anti-NR1 polyclonal antibody plus blocking peptide, and subjected to immunoblot analysis using anti-NR1 or anti-CaM monoclonal antibodies. In (A)–(D), arrowheads indicate immunoprecipitated NR1 protein and arrows indicate CaM. Molecular mass markers in kilodaltons are shown.

were performed on lysates of QT6 cells expressing both NR1 and NR2B subunits using an anti-NR2B antibody. No CaM was observed to coprecipitate with NR2B subunits from cells expressing NR2B alone (Figure 2C), although NR2B expression was detectable by immunoblot (data not shown). However, CaM did coprecipitate with NR2B from cells expressing both NR1a and NR2B (Figure 2C). This coprecipitation was likely due to an indirect association of CaM with NR2B through the NR1a subunit, as both NR1a and CaM were detected in anti-NR2B coimmunoprecipitates from NR1a/NR2B coexpressing cells (Figure 2C). Substitution of NR1c for NR1a in the heteromeric receptor complex abolished CaM coprecipitation, even though NR1c coprecipitated with NR2B in amounts roughly equal to that of NR1a (Figure 2C). These experiments showed that CaM associates with heteromeric NMDA receptor complexes through interaction with the NR1 subunit, and that this interaction is regulated by the presence of the C1 exon cassette.

CaM was also found to coimmunoprecipitate with NR1 subunits from adult rat cortex (Figure 2D). This coimmunoprecipitation was blocked by both preincubation of the anti-NR1 antibody with excess immunogenic peptide, and by removal of Ca^{2+} and addition of EGTA (Figure 2D). No CaM was observed to precipitate when preimmune serum was substituted for anti-NR1 antibody (Figure 2D). These data indicated that NMDA receptors present in the brain also associate with Ca^{2+}-CaM.

Quantitative Analysis of CaM Binding to the COOH-Terminus of NR1a and NR1c

To quantitate the binding of CaM to NR1 subunits, fluorimetry was performed on solutions of dansyl-CaM titrated with NR1a COOH-terminal (NR1a-Cterm) and NR1c COOH-terminal (NR1c-Cterm) fusion proteins (see Figure 1C) (Kincaid et al., 1982; Liu et al., 1994). Details of the method are described in Experimental Procedures. The photoexcited emission spectrum of dansyl-CaM (200 nM) alone had a maximum at 498 nm (Figure 3A). Addition of 200 nM NR1a-Cterm shifted the emission spectrum maximum to 480 nm and increased the fluorescence intensity by a factor of 1.53 (Figure 3A). Addition of 200 nM NR1c-Cterm shifted the emission spectrum maximum to 474 nm and increased the fluorescence intensity by a factor of 1.36 (Figure 3A). This spectral shift provided a means of quantitating the CaM binding by titrating the dansyl-CaM with fusion protein and measuring the fractional fluorescence increase at 480 nm (Kincaid et al., 1982; Liu et al., 1994).

Measurement of the fractional fluorescence increase of dansyl-CaM upon titration with NR1a COOH-terminal fusion protein showed that NR1a binds CaM with high affinity (Figure 3B). Scatchard analysis of the data revealed a curvilinear Scatchard plot (Figure 3B). The curved nature of the data suggested that the COOH-terminus of NR1a might contain two separate CaM binding sites with different affinities for CaM. The negative

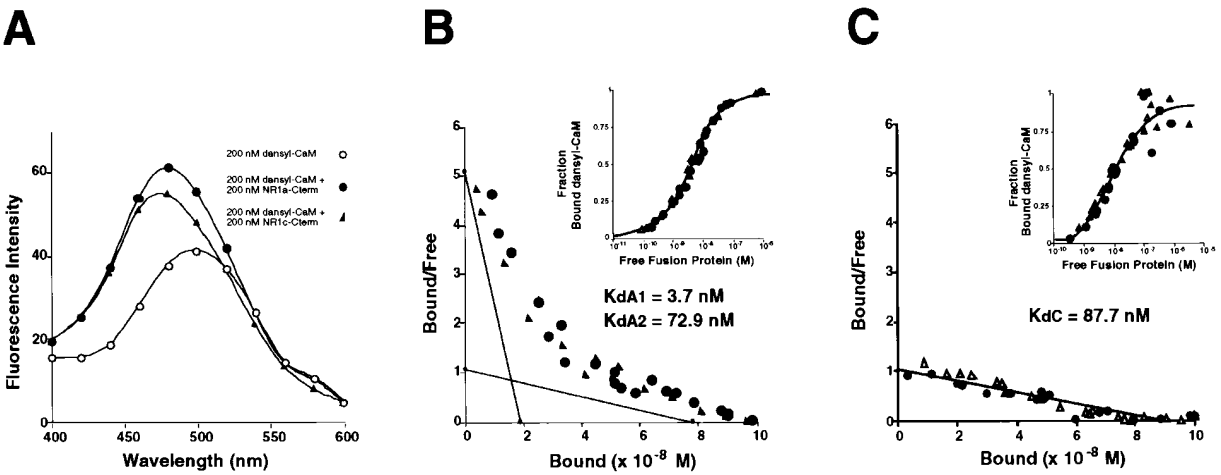

Figure 3. Quantitative Measurement of CaM Binding to COOH-Terminal Fusion Proteins

(A) Emission fluorescence spectra of dansyl-CaM alone (open circles), dansyl-CaM + NR1a-Cterm (closed circles), and dansyl-CaM + NR1c-Cterm (triangles).

(B and C) Quantitative analysis of CaM binding to NR1a-Cterm (B) and NR1c-Cterm (C) fusion proteins. Scatchard plots of bound dansyl-CaM/free dansyl-CaM versus bound dansyl-CaM are shown along with the lines fit to the data using the two binding site (B), or single binding site (C) Scatchard relationship. The insets show saturation plots of the fraction of bound dansyl-CaM versus free NR1a-Cterm (B, inset) or free NR1c-Cterm (C, inset) fusion protein. Data from two experiments are shown in each case.

reciprocal slopes of the lines gave dissociation constants of 3.7 nM and 72.9 nM. In addition, saturation of NR1a-Cterm/dansyl-CaM binding occurred over ~2.7 log units, providing further evidence for two binding sites (Figure 3B, inset).

Similar analysis of dansyl-CaM binding to the NR1c COOH-terminal fusion protein revealed a more linear Scatchard plot (Figure 3C), with saturation of NR1c-Cterm/dansyl-CaM binding occurring over approximately two log units (Figure 3C, inset). These data supported a single binding site model for NR1c-Cterm. The negative reciprocal slope of the fit line in the Scatchard plot gave a dissociation constant of 87.7 nM, which is close to that of the low affinity CaM binding site of NR1a-Cterm (72.9 nM). These experiments demonstrated that the COOH-termini of NR1a and NR1c bind CaM with somewhat different affinities, with NR1a-Cterm having a higher apparent affinity for CaM than NR1c-Cterm. Moreover, these data suggested that the COOH-terminus of NR1a might contain two CaM-binding sites, one of high affinity and one of lower affinity, with the high affinity site being dependent on the presence of the C1 exon cassettte, possibly within the cassette itself.

Identification and Quantitative Analysis of CaM Binding Domains in the NR1 Subunit

Analysis of the amino acid sequence of the COOH-terminus of NR1a revealed two prominent stretches of basic and hydrophobic amino acids as two possible CaM binding sites (James et al., 1995). The first site comprises amino acids (aa) 838–863, corresponding to the region of the NR1 COOH-terminus between putative transmembrane domain IV and the C1 cassette. The second site comprises aa 875–898, corresponding to a region wholly contained within the C1 cassette. Two synthetic peptides (RH106 and RH96) were synthesized that correspond to these two regions (RH106[aa 838–863]: KRHKDARRKQMQLAFAAVNVWRKNLQ; RH96[aa 875–898]: KKKATFRAITSTLASSFKRRRSSK) (Figure 4A). Preincubation of CaM with either peptide in the presence of Ca^{2+} shifted CaM's mobility on a nondenaturing polyacrylamide gel (Figures 4B and 4C), indicating the formation of stable peptide–CaM complexes. Removal of Ca^{2+} by the addition of EGTA abolished the gel shift, and preincubation of CaM with peptides corresponding to other NMDA receptor sequences had no effect on CaM's gel mobility (data not shown). Increasing the peptide:CaM molar ratio for both RH106 and RH96 resulted in an increasingly complete shift of CaM to the peptide-bound form, with complete shifts occurring at peptide:CaM ratios of ~10:1 and 2:1 for RH106 and RH96, respectively (Figures 4B and 4C). These results demonstrated that both RH106 and RH96 peptides were capable of binding CaM, and suggested that the RH96 peptide had a higher affinity for CaM than the RH106 peptide.

To quantitate the binding of CaM to RH96 and RH106, fluorimetry experiments were performed on solutions of dansyl-CaM titrated with RH96 and RH106 peptides. Data obtained from these experiments showed that RH96 and RH106 bind CaM with different affinities (Figures 4D and 4E). The negative reciprocal slopes of the Scatchard plots (Figures 4E) gave dissociation constants of 4.0 nM for RH96 and 87.0 nM for RH106. The data from two separate experiments are shown. The affinity of RH96 (4.0 nM) for CaM correlates well with that of the high affinity site of the NR1a COOH-terminal fusion protein (3.7 nM), and the affinity of RH106 (87.0 nM) for CaM correlates well with those of the low affinity site of the NR1a COOH-terminal fusion protein (72.9 nM) and the NR1c COOH-terminal fusion protein (87.7 nM). These results showed that the COOH-terminus of the NR1 subunit of the NMDA receptor contains two separate CaM binding sites with different affinities for CaM,

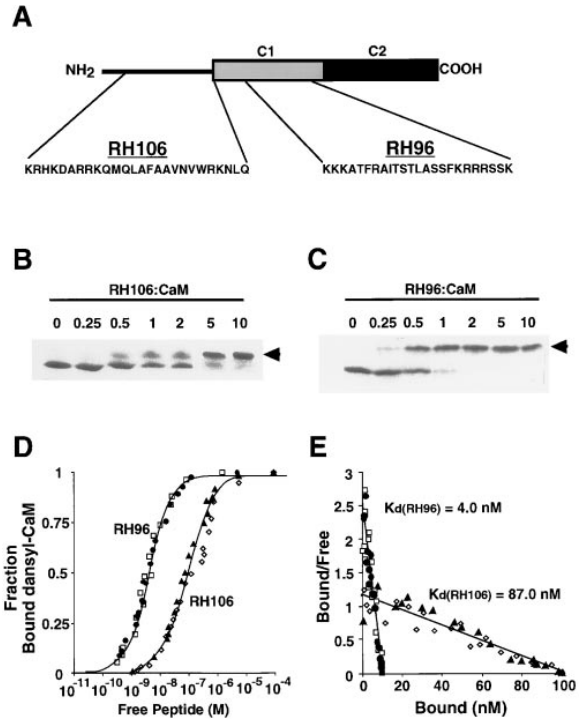

Figure 4. Identification and Quantitative Analysis of CaM Binding Domains in the NR1 COOH-Terminus

(A) Schematic diagram of the COOH-terminal domain of NR1a from putative transmembrane domain IV to the COOH-terminus (amino acids 834–938).

(B and C) CaM (300 pmol) was incubated with varying molar amounts of RH106 (B) and RH96 (C) peptides and the peptide/CaM complexes resolved on a 15% nondenaturing polyacrylamide gel and visualized by Coomassie blue staining. Arrowheads indicate peptide/CaM complexes.

(D and E) Quantitative analysis of CaM binding to RH106 and RH96 peptides. Saturation plots of the fraction of bound dansyl-CaM versus free peptide are shown in (D), and Scatchard plots of bound dansyl-CaM/free dansyl-CaM versus bound dansyl-CaM are shown in (E) along with curves fit to the data from two separate experiments in each case (open squares and closed circles, RH96; open diamonds and closed triangles, RH106).

with the high affinity CaM binding site being present only in C1 cassette–containing NR1 splice variants.

Ca^{2+}-CaM Inhibits NMDA Receptor Channel Currents by Reducing the Channel's Open Rate and Mean Open Time

To explore the functional consequences of direct binding of CaM to NR1 subunits, we examined the effect of CaM on the channel properties of recombinant NMDA receptors consisting of NR1 and NR2A subunits using inside-out patch-clamp recording techniques. The inside-out patch configuration allowed access to COOH-terminal domains of NR1 subunits present in the NMDA receptor complex. Indirect effects of cytoplasmic factors such as Ca^{2+}-CaM-dependent protein kinases were minimized by using cell-free membrane patches in the absence of Mg^{2+} and ATP. When the patch pipettes contained a low concentration of NMDA or glutamate (0.5–2 μM) and saturating levels of glycine (10 μM; Vc = 60 mV, equal concentration of Na^+ on both sides as the major current carrier), NR1a-NR2A recombinant NMDA channel opening events occurred with a primary conductance level of 56 pS and a subconductance level of 42 pS with transitions occurring between these two open states (Figure 5A). A 21 pS conductance level was also observed in some experiments. Channel activity increased with increasing NMDA concentration and was blocked by perfusion of 200 μM DL-2-amino-4-phosphonovaleric acid into the patch pipette (data not shown). Moreover, no similar channel events were observed from untransfected HEK 293 cells.

In each experiment, the cytoplasmic face of the membrane patch was perfused with solutions varying in Ca^{2+} and CaM concentration and NMDA channel events recorded under voltage clamp. Before application of CaM, membrane patches were perfused with a calcium-free solution in order to establish the control level of channel activity (Figure 5A). Application of CaM (2–250 nM) in the presence of 50 μM Ca^{2+} to the cytoplasmic face of the patch substantially reduced the single NMDA channel activity (Figure 5B). This Ca^{2+}-CaM-dependent decrease in channel activity was reversed by perfusion with 0 Ca^{2+} solution (Figure 5C). Due to the slow, Ca^{2+}-CaM-independent rundown of NMDA currents, the channel activity was not completely restored to the initial control value (Figure 5C; see below). Perfusion of CaM in the absence of Ca^{2+} (data not shown) or Ca^{2+} in the absence of CaM (Figure 5D) had no effect on channel activity. Moreover, preincubation of Ca^{2+}-CaM with a CaM inhibitor peptide (Liu et al., 1994) abolished CaM's effect on NMDA channel activity ($n = 6$).

Analysis of single NMDA channel records showed that CaM did not cause any apparent change in NMDA channel conductance levels (Figures 5 and 6A). However, open time histograms of single NMDA channel records revealed that CaM causes an overall decrease in the number of opening events (reduction in histogram amplitude), and a reduction in the mean channel open time (leftward shift of histogram mean) (Figure 6B). Data collected from 8 patches presumably containing single NMDA channels (no simultaneous openings observed) showed that the open rate was reduced to 38% of the control level of 2.05/s, and the mean open duration was shortened to 53% of the control level of 6.03 ms (Figure 6C). As a result, the probability of NMDA channels being open during CaM administration (0.00378) was 4-fold less than during 0 Ca^{2+} perfusion (0.0151; Figure 6C). To correct for the slow process of CaM-independent channel rundown, control values were taken as an average of those measured during 0 Ca^{2+} perfusions both before and after CaM application. Only patches that showed reversibility of the CaM-dependent inactivation were used for analysis. These experiments demonstrated that both the open rate and mean open duration of NMDA channels could be markedly reduced by nanomolar concentrations of CaM in a Ca^{2+}-dependent manner.

The Presence of CaM Binding Sites in NR1 Determines the Sensitivity of NMDA Channels to CaM Inhibition

To test whether the inhibition of NMDA channel activity by CaM resulted from direct binding of CaM to the two

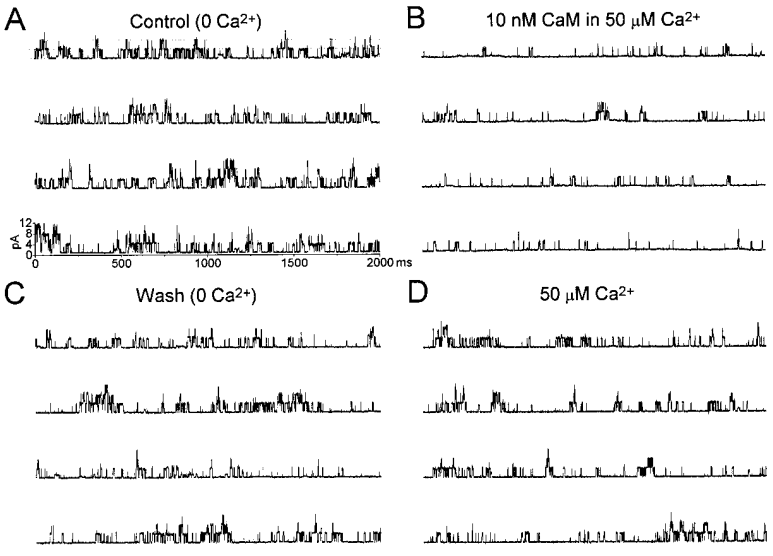

Figure 5. Ca^{2+}-CaM Inhibits the Activity of NMDA Receptor Channels

(A)–(D) represent portions of a recording of NMDA channel currents (upward events; Vc = 60 mV) from a single inside-out membrane patch excised from an HEK 293 cell transfected with cDNAs encoding NR1a and NR2A subunits. Different experimental conditions are shown sequentially in each panel. The time and amplitude scales shown in (A) also apply to (B)–(D).

(A) Continuous 8 s recording of NMDA channel currents under control conditions where the cytoplasmic side of the patch was perfused with a Ca^{2+}-free buffer containing 1 mM EGTA. The baseline and primary conductance levels are indicated by dotted lines.

(B) When 10 nM CaM in 50 μM Ca^{2+} was perfused onto the cytoplasmic face of the patch, the NMDA channel currents were reduced.

(C) The inhibitory effect was reversed by washing with Ca^{2+}-free buffer containing 1 mM EGTA.

(D) The inhibitory effect was not due to Ca^{2+} ions alone as perfusion with 50 μM Ca^{2+} without CaM did not inhibit channel activity.

sites in the COOH-terminus of the NR1 subunit, we examined the effect of deleting various regions of the NR1 COOH-terminus on CaM-dependent inactivation (Figure 7). The effect of CaM on NMDA receptors was quantitated by integrating currents to calculate the total electrical charge passing through open channels in equal amounts of time during either 0 Ca^{2+} perfusion or perfusion of various concentrations of CaM with 50 μM Ca^{2+}. For each patch, the total charge during administration of CaM was normalized to the control value (taken as the average value of total charge passed during 0 Ca^{2+} perfusions both before and after CaM application). Data from multiple patches with the same NR1 construct at identical concentrations of CaM were averaged to obtain dose–response curves.

The dose–response curves for CaM-dependent inactivation of NMDA receptors composed of each of 5 different NR1 splice variants and deletion mutants along with the NR2A subunit are shown in Figure 7. NMDA channels containing NR1a showed the greatest sensitivity to CaM. At a CaM concentration of 2 nM, NMDA channel activity was maximally inhibited by 4- to 5-fold (Figure 7). Truncation of the COOH-terminus of NR1 immediately after transmembrane domain IV completely abolished the CaM-dependent inactivation (Figure 7). NR1c- and NR1e-containing NMDA receptors were less sensitive to CaM, with CaM still maximally reducing the total charge passed by 4- to 5-fold, but only at a higher CaM concentration (10 nM; Figure 7). This lower sensitivity to CaM could be completely abolished by deleting aa 839–863 of NR1c (Figure 7). These data are consistent with the biochemical identification of two CaM binding sites in the COOH-terminus of the NR1 subunit with differing affinities for CaM. NR1a possesses both CaM binding sites and NR1a-containing NMDA receptors are sensitive to CaM-dependent inactivation at CaM concentrations close to the K_d for high affinity binding (Figures 4 and 7). NR1c and NR1e splice variants both lack the high affinity CaM binding site (since both lack the C1 cassette), but contain the lower affinity CaM binding site, and NMDA receptors containing these NR1 subunits are sensitive to CaM only at higher CaM concentrations. Deleting both CaM binding sites in the NR1 subunit (NR1-stop834 and NR1c-839–863) completely abolished CaM's inhibitory effect. These results, taken together with the biochemical data, demonstrate that CaM acts to inactivate NMDA receptors by directly binding to specific sites within the COOH-terminus of the NR1 subunit.

Discussion

In this study, we have shown that the multifunctional Ca^{2+} sensor protein CaM directly binds to and inactivates NMDA receptor channels. CaM acts by binding to two separate sites in the COOH-terminus of the NR1 subunit. The dose response of CaM-dependent inactivation of NMDA channels containing NR1 subunits with differing COOH-terminal domains parallels the measured affinity of CaM for the two binding sites. The quantitative differences between measured biochemical affinities and physiological dose response could be due to a higher affinity of CaM for these sites in the native receptor relative to that seen in vitro. Also, because NMDA receptors are multimeric complexes likely to contain multiple NR1 subunits, CaM-dependent inactivation might occur when CaM binds to only a single NR1 subunit in the complex, leading to a higher apparent affinity in the physiological dose response. Both CaM binding sites in the NR1 subunit possess stretches of basic and hydrophobic residues that segregate to opposite faces of a theoretical α helix, a hallmark of CaM binding domains (James et al., 1995). The result of CaM binding is a reduction in both the opening frequency and mean open time of individual NMDA channels.

Given the Ca^{2+}-permeable nature of NMDA receptors, our data suggest a model whereby activation of NMDA receptors by glutamate causes an influx of Ca^{2+} through the NMDA channel that activates CaM, allowing CaM to

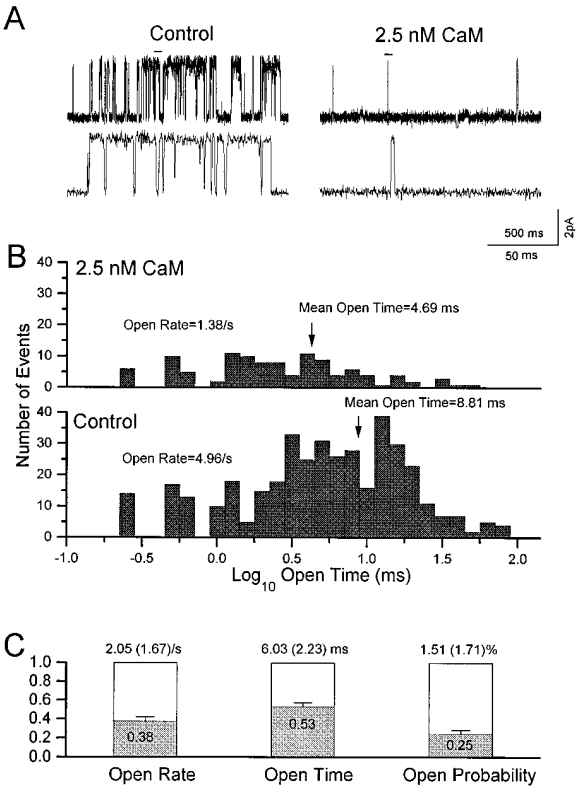

Figure 6. Ca^{2+}-CaM Reduces the Open Rate and Open Duration of NMDA Channels

(A) Examples of single channel events of an isolated NMDA receptor (inside-out patch, Vc = 60 mV) when bathed with 0 Ca^{2+} (left) and 2.5 nM CaM with 50 μM Ca^{2+} (right). Brief periods of the upper panels (marked with bars) are expanded in the lower panels.

(B) Open time histograms (log_{10} values) of the NMDA channel in (A) during two 80 s recording periods. The open time histogram of single channel events during perfusion of the cytoplasmic face of the patch with a Ca^{2+}-free buffer containing 1 mM EGTA is shown in the lower panel. Perfusion with 2.5 nM CaM plus 50 μM Ca^{2+} resulted in a reduction in both the open rate and mean open time of the NMDA channel (top histogram). Channel open rates and mean open times under both conditons are shown.

(C) The channel open rate, mean open time, and open probability of single NMDA receptors (NR1a/2A, n = 8) in the presence of Ca^{2+}-CaM (2–200 nM CaM; shaded areas in the bars) normalized to control values in the absence of Ca^{2+}-CaM. Means and standard deviations (in parentheses) of the control values are indicated above the boxes. Error bars in the shaded areas indicate standard error.

bind directly to two possible sites in the COOH-terminus of the NR1 subunit, resulting in inactivation of the channel (Figure 8). Still unknown is the precise gating mechanism by which CaM inactivates NMDA channels. Also unknown is the degree of cooperativity between the two CaM binding sites in the NR1 subunit, and whether CaM binding to each site subserves the same physiological function, or whether CaM binding to the high affinity site in the C1 cassette serves only to enhance CaM's effect at the low affinity site. It is interesting to note that the binding of Ca^{2+}-CaM to a defined site in the NH_2-terminus of the olfactory cyclic nucleotide–gated cation channel also reduces channel activity (Chen and Yau, 1994; Liu et al., 1994). Direct CaM binding might thus be a

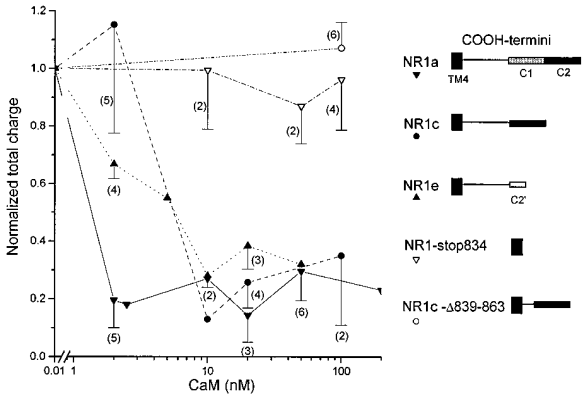

Figure 7. The Sensitivity of NMDA Receptor Channels to CaM Depends on the Presence of the Two CaM Binding Sites in the COOH-Terminus of the NR1 Subunit

The total electrical charge passing through open NMDA channels (NR1/NR2A) during Ca^{2+}-CaM perfusion is normalized to the control level and plotted against the concentration of CaM. For each NR1 construct and CaM concentration, data from multiple patches were averaged to obtain the mean (points) and standard error (error bars). Sample sizes are indicated in parentheses. Structures of the COOH-terminal domains of the five different NR1 constructs are shown on the right. C1 and C2 indicate exon cassettes; C2′ indicates the alternative COOH-terminus generated by removal of the C2 exon cassette; TM4 indicates putative transmembrane domain IV.

general mechanism for Ca^{2+}-dependent regulation of ion channel properties.

The C1 Exon Cassette as a Multifunctional Regulatory Domain

The 37 aa C1 exon cassette has become increasingly recognized as a site of significant functional regulation of NMDA receptors. The C1 cassette serves as a substrate for protein phosphorylation by both protein kinase

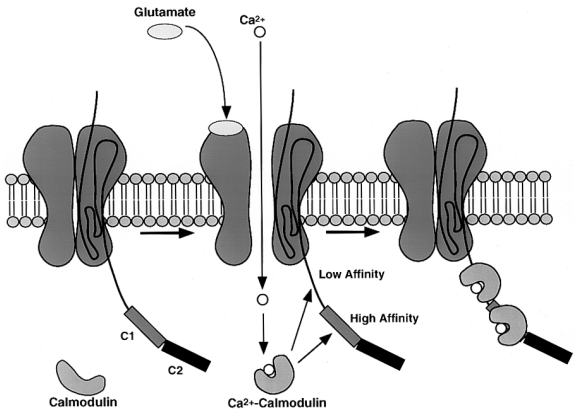

Figure 8. Schematic Diagram Illustrating Proposed Model of Calmodulin-Dependent NMDA Receptor Inactivation

In this simplified model, activation of NMDA receptors by glutamate (in conjunction with postsynaptic depolarization) leads to an influx of Ca^{2+} ions through the channel. Binding of Ca^{2+} to nearby CaM allows CaM to bind directly to the receptor through either the low affinity or high affinity sites in the COOH-terminus of the NR1 subunit. The binding of CaM results in inactivation of the NMDA receptor channel.

C (PKC) (Tingley et al., 1993) and protein kinase A (PKA) (Tingley and Huganir, unpublished data). Moreover, the C1 cassette targets recombinant NR1 subunits to receptor-rich domains in cultured cell lines, presumably owing to the interaction of this domain with the cytoskeleton (Ehlers et al., 1995). In this study, we have shown that the C1 cassette also contains a high affinity binding site for CaM.

Sequence comparison with other known CaM binding sites reveals a striking homology between the high affinity CaM binding site of NR1 and the multifunctional CaM binding site (effector domain) of the cytoskeletal organizing protein MARCKS (myristoylated alanine-rich C-kinase substrate; for review, see Aderem, 1992). MARCKS is a major cellular substrate of PKC that binds both CaM and actin and is thought to mediate reversible attachment of the actin cytoskeleton to the plasma membrane. The 18 aa effector domain of the MARCKS protein not only binds CaM, but also binds actin, and is the major site of PKC phosphorylation. These three processes display extensive interaction, with PKC phosphorylation inhibiting CaM- and actin-binding, and CaM-binding preventing PKC phosphorylation and actin-binding.

As with the MARCKS protein, several observations suggest that the processes of CaM binding, protein phosphorylation, and cytoskeletal association of the NR1 subunit of the NMDA receptor may functionally interact. Phosphorylation of serines within the C1 cassette rapidly disperses NR1-rich domains in cultured cells (Ehlers et al., 1995), possibly by disrupting the interaction of the C1 cassette with the cytoskeleton. Studies by Rosenmund and Westbrook (1993b) have demonstrated that NMDA receptor linkage to the actin cytoskeleton can regulate Ca^{2+}-dependent desensitization of the receptor, perhaps by competitive binding of Ca^{2+}-CaM and cytoskeletal elements to the C1 cassette. Preliminary results suggest that protein phosphorylation and CaM binding at the high affinity CaM binding site in C1 are mutually antagonistic (Ehlers and Huganir, unpublished data), consistent with the observation that the high affinity site in C1 overlaps with known phosphorylation sites (Tingley et al., 1993). Together, these observations suggest that the C1 exon cassette may serve as a multifunctional regulatory domain affecting both NMDA channel physiology and cytoskeletal association in a manner analogous to the MARCKS protein.

Ca^{2+}-CaM Binding to the NR1 Subunit as a Mechanism for Ca^{2+}-Dependent Inactivation of NMDA Receptors

Intracellular Ca^{2+} exerts a negative regulatory effect on neuronal and recombinant NMDA channels (Mayer and Westbrook, 1985; Zorumski et al., 1989; Legendre et al., 1993; Vyklicky, 1993; Medina et al., 1995). In neurons, Ca^{2+} influx through NMDA channels is more effective than influx through voltage-gated Ca^{2+} channels in mediating Ca^{2+}-dependent NMDA channel inactivation (Legendre et al., 1993), suggesting that the site of action of Ca^{2+} is near the cytoplasmic face of the NMDA channel itself. Consistent with these studies is our finding that CaM binds directly to the cytoplasmic COOH-terminus of the NR1 subunit and inactivates NMDA channels in a Ca^{2+}-dependent manner. This CaM-dependent inactivation could account for some or all of the Ca^{2+}-dependent inactivation observed by whole-cell and cell-attached patch recordings. Recent experiments have also indicated a role for the Ca^{2+}-CaM-dependent phosphatase calcineurin in NMDA receptor desensitization (Lieberman and Mody, 1994; Tong et al., 1995). It is tempting to speculate that calcineurin might act in part by dephosphorylating the NR1 subunit at sites within the C1 cassette, making available the high affinity CaM binding site and allowing for rapid CaM-dependent NMDA receptor inactivation.

CaM-Dependent Inactivation of NMDA Receptors and Control of Intracellular Ca^{2+}

Ca^{2+} serves as a major intracellular messenger in the processes of synaptic plasticity, neuronal development, and excitotoxicity. Ca^{2+} influx into the dendritic spine through NMDA channels is critical for establishing both long-term potentiation (LTP) and long-term depression (LTD) of synaptic strength (Bliss and Collingridge, 1993; Bear, 1995). The magnitude of the postsynaptic Ca^{2+} concentration increase determines the nature of the change in synaptic efficiency, with low Ca^{2+} levels resulting in LTD and high Ca^{2+} levels resulting in LTP (Bear, 1995). In addition, excessive Ca^{2+} influx through NMDA receptors can result in neuronal death (Choi, 1995). CaM-dependent inactivation of NMDA channels could provide one mechanism for negative feedback regulation of activity-dependent Ca^{2+} influx into the postsynaptic spine. Such inactivation might protect against excitotoxic cell death. Furthermore, regulation of this negative feedback mechanism by protein phosphorylation or alternative splicing would provide effective control over Ca^{2+} levels in the dendritic spine and thus potentially affect the balance between LTP and LTD.

Experimental Procedures

Transfection and Metabolic Labeling of QT6 Cells

HEK 293 cells and QT6 cells were transfected with cDNAs for CD8, NR1a, NR1c, NR1e, NR2A, NR2B, as well as mutant NR1-stop834 and NR1c-839–863 subcloned into an expression vector containing the CMV promoter (20 μg/100 mm plate; 8 μg/60 mm plate) as indicated using calcium phosphate coprecipitation as described (Ehlers et al., 1995). For metabolic labeling, transfected QT6 cells were incubated in cysteine- and methionine-free minimum essential medium with 1 mCi/ml ^{35}S-TransLabel (ICN) for 4 hr at 37°C. The media used was Media 199 with 10% tryptose phosphate broth, 5% fetal bovine serum, and 1% dimethylsulfoxide for QT6 cells, and minimum essential medium with 10% fetal bovine serum and 10 mM sodium pyruvate for HEK 293 cells. For coexpression of NR1 and NR2 subunits, either 100 μM MK-801 or 0.5 mM DL-2-amino-4-phosphonovaleric acid was added to the media.

Coimmunoprecipitation of Proteins Associated with NMDA Receptor Subunits from Transfected QT6 Cells

Transfected QT6 cells were solubilized for 30 min at 4°C in either buffer A (50 mM Tris–HCl [pH 8.0], 500 mM NaCl, 2 mM $CaCl_2$, 1% Nonidet P-40 [Sigma], containing protease inhibitor mix: [100 μM phenylmethylsulfonylfluoride {PMSF}, and 10 μg/ml each of leupeptin, antipain, chymostatin, and pepstatin]) for NR1-expressing cells, or buffer B (50 mM Tris–HCl [pH 8.0], 150 mM NaCl, 2 mM $CaCl_2$, 1% Nonidet P-40, containing protease inhibitor mix) for cells expressing both NR1 and NR2 subunits. In some experiments, 5 mM EGTA was substituted for 2 mM $CaCl_2$ in buffers A and B as indicated. Soluble

cell lysates were immunoprecipitated using previously described anti-NR1 (Tingley et al., 1993) or anti-NR2B (Lau and Huganir, 1995) polyclonal antibodies and protein A–sepharose for 2 hr at 4°C. Coimmunoprecipitates were washed with buffer A or buffer B, eluted with sample buffer, resolved by SDS–polyacrylamide gel electrophoresis (SDS–PAGE), and visualized by fluorography (Entensify, NEN) or transferred to a polyvinylidene fluoride (PVDF) membrane (Immobilon-P, Millipore) and visualized by immunoblot analysis with enhanced chemiluminescence (ECL) detection (DuPont). Immunoblots were performed as described previously (Blackstone et al., 1992) using an anti-CaM antibody (UBI; 1:2,000 dilution) or anti-NR1 54.1 monoclonal antibody (Pharmingen; 1:50,000 dilution).

In Vitro Binding of Metabolically Labeled QT6 Cell Proteins and CaM to COOH-Terminal NR1 Fusion Proteins

Previously described hexahistidine-tagged fusion proteins corresponding to the COOH-termini of NR1a (aa 834–938), the COOH-terminus of NR1c (aa 834–901) (Tingley et al., 1993), and the hexahistidine backbone fusion protein were coupled to Affigel (BioRad). Either soluble lysates from metabolically labeled QT6 cells or 1 μg of CaM (Calbiochem) was incubated with 50 μl bed volume of fusion protein-Affigel resin in a total volume of 1 ml of buffer A, buffer B, or radio immunoprecipitation assay (RIPA) buffer (50 mM Tris–HCl [pH 8.0], 150 mM NaCl, 2 mM $CaCl_2$, 1% Nonidet P-40, 0.5% deoxycholate, 0.1% SDS, containing protease inhibitor mix) for 2 hr at 4°C. In some experiments, 5 mM EGTA was substituted for 2 mM $CaCl_2$ as indicated. The resin was washed with buffer A, buffer B, or RIPA buffer, and the bound proteins eluted with protein sample buffer, resolved by SDS-PAGE, and visualized by autoradiography or immunoblot analysis (Blackstone et al., 1992) using an anti-CaM antibody (UBI) (1:2000 dilution).

Purification and Microsequencing of a 20 kDa Protein from QT6 Cells that Associates with the COOH-Terminus of NR1

Twenty 100 mm plates of QT6 cells were solubilized in buffer A for 30 min at 4°C and the soluble supernatant incubated with 1 ml bed volume of Affigel resin coupled to NR1a COOH-terminal fusion protein for 2 hr at 4°C as described above. Proteins bound to the NR1a affinity resin were eluted with sample buffer, resolved by SDS-PAGE, and transferred to a PVDF membrane. Proteins present on the membrane were visualized by amido black staining. The prominent 20 kDa protein present in the sample was cut from the membrane and microsequenced at the Wistar Protein Microchemistry Laboratory (Philadelphia, PA) by performing in situ proteolysis on the PVDF membrane followed by microbore reverse phase high performance liquid chromatography and internal sequence analysis on isolated peptide fractions.

Coimmunoprecipitation of CaM with NR1 Subunits from Rat Brain

Cortex from adult Sprague-Dawley rats was homogenized on ice in 50 mM Tris-HCl (pH 8.0), 500 mM NaCl, 2 mM $CaCl_2$ containing protease inhibitor mix using a Brinkman Polytron PT 3000. Due to the low solubility of NMDA receptor subunits in nonionic detergents, 3 mg of cortex protein was used for each coimmunoprecipitation experiment. Cortex homogenate was solubilized by adding Nonidet P-40 to 1% and incubating at 4°C for 30 min. Homogenates were then incubated with either preimmune serum, polyclonal anti-NR1 antibody, or polyclonal anti-NR1 antibody + 100 μg/ml blocking peptide along with protein A-sepharose for 2 hr. Bound complexes were then washed and eluted as described above for transfected QT6 cell lysates. The coimmunoprecipitates were resolved by SDS-PAGE, transferred to a PVDF membrane, and subjected to immunoblot analysis using anti-NR1 54.1 monoclonal antibody (Pharmingen) (1:50,000 dilution) or anti-CaM antibody (UBI) (1:2000 dilution).

Quantitative Fluorescence Measurements of CaM Binding

Emission fluorescence spectra of dansyl-CaM alone, dansyl-CaM with either NR1a- or NR1c-COOH terminal fusion proteins, and dansyl-CaM with either RH96 or RH106 peptides were measured with a Perkin–Elmer LS50B luminescence spectrometer. The excitation wavelength was 340 nm and both excitation and emission bandpasses were 15 nm. All experiments were performed in a buffer containing 50 mM Tris–HCl (pH 7.4), 150 mM NaCl, and 2 mM $CaCl_2$. Measurements of dansyl-CaM binding to NR1a- and NR1c-COOH terminal fusion proteins, as well as to RH106 peptide, were taken on samples containing 100 nM dansyl-CaM in the above buffer into which portions of concentrated fusion protein or peptide solution were sequentially added. For measurements of dansyl-CaM binding to RH96 peptide, the initial concentration of dansyl-CaM was 10 nM. The resulting dilution of the original dansyl-CaM solution was less than 4% for measurements of fusion protein binding, and less than 1% for measurements of peptide binding. The fraction of bound dansyl-CaM was calculated from the fractional fluorescence increase at 480 nm using the relationship $I_m = I_f(1-f_b) + I_b f_b$, or rearranging, $f_b = (I_m - I_f)/(I_b - I_f)$ where I_f is the fluorescence if all dansyl-CaM is free, I_b is the fluorescence if all dansyl-CaM is bound, I_m is the measured fluorescence for any arbitrary intermediate mixture of the two, and f_b is the fraction of bound dansyl-CaM. From these values, the concentrations of bound dansyl-CaM, bound fusion protein, free dansyl-CaM, and free fusion protein could be determined and used to construct Scatchard plots and saturation curves. Lines were fit to the data using either the single site Scatchard relationship $B/F = -B/K_d + B_{max}/K_d$ or the two site Scatchard relationship $B/F = B^1_{max}/(K^1_d + F) + B^2_{max}/(K^2_d + F)$ as appropriate, where B is the amount bound, F is the amount free, K_d is the dissociation constant for each separate site, and B_{max} represents the maximal number of binding sites for each site. Dissociation constants were determined from the Scatchard plots as the negative reciprocal of the slope of the line(s) fit to the data by the least squares method.

Nondenaturing Polyacrylamide Gel-Shift Assays of CaM-Peptide Complexes

Three hundred picomoles of CaM were incubated with different molar amounts of either RH96 or RH106 peptide in a buffer containing 10 mM sodium-HEPES (pH 7.5) and 2 mM $CaCl_2$ for 30 min at room temperature. The bound complexes were then resolved by nondenaturing PAGE on a 15% polyacrylamide gel in the presence of 2 mM $CaCl_2$, and visualized by Coomassie blue staining.

Site-Directed Mutagenesis of NR1 cDNA

Mutations in the NR1 cDNA were introduced using double stranded site-directed mutagenesis (Chameleon system, Strategene) as per the manufacturer's instructions. Mutations were confirmed by sequencing, and expression of NR1 mutants was verified by transfection and immunoblot analysis as described above. The mutagenic antisense oligonucleotides used were as follows: 5′GTGTCGCTTGT AAGCTTACTAAATGAAAATGAGG-3′ for NR1-stop834, which introduces stop codons at aa positions 834 and 835 immediately following putative transmembrane domain IV, and 5′-GCGTCCACCCCCG GTCGACTTGTAGGCGATCTC-3′ for NR1c-839–863, which deletes aa 839–863 from NR1C.

Electrophysiology

Ionic currents through single NMDA receptors were recorded from inside-out patches excised from transiently transfected human embryonic kidney cells (HEK 293). For visual identification, the expression plasmid πH3-CD8 (gift from Brian Seed) was cotransfected with NR1 and NR2A (1:4.5:4.5 ratio of CD8:NR1:NR2A cDNA). After 24–72 hr, transfected cells were visualized with magnetic polystyrene microspheres coated with antibodies to CD8 (M-450 CD8, Dynal, Inc.). Inside-out patches were excised from bead-bearing cells with pipette electrodes made from Corning 7052 glass capillaries of 1.5 mm o.d. and 0.75 mm i.d. (Warner Instrument Corp.) by a Sachs-Flaming micropipette puller (PC-84, Sutter Instrument Co.). The pipettes were coated with Sylgard 184 silicone (Dow Corning) near their tips, which were then heat polished. The osmolarity of the extracellular and intracellular solutions (290–310 mmol/kg) was verified using a 5500 vapor pressure osmometer (Vescor, Inc.). The pipette filling solution contained 0.5–2 μM NMDA or glutamate and 10 μM glycine in a calcium-free buffer containing 145 mM NaCl, 10 mM HEPES, and 1 mM EGTA, pH 7.4 (EM Science). Impedance of the pipette electrodes was 4 to 8 MΩ. Cytoplasmic faces of isolated

patches were perfused with either the calcium-free buffer or a buffer containing 50 μM Ca^{2+} (145 mM NaCl, 10 mM HEPES, 2 mM nitrilotriacetic acid, 0.7 mM $CaCl_2$, pH 7.4) through glass theta tubing, which was placed 1.8 mm from the patches. The free Ca^{2+} was calculated as 50 μM based on nitrilotriacetic acid–Ca^{2+} complex equilibrium constants. The perfusion flow rate was 0.25 ml/min. The membrane patches were voltage-clamped at 60 mV with an Axopatch 200 amplifier (Axon Instruments). Single channel currents were low-pass filtered at 1 kHz and stored on video tapes with a PCM VCR (DAS 900, Unitrade, Inc.) for later digitizing (sampling rate = 5 kHz) and data analysis, using Digidata 1200 hardware and pClamp6 programs (Axon Instruments). All experiments were carried out at room temperature (20°C–23°C).

Acknowledgments

The authors thank D. Speicher and D. Reim at the Wistar Protein Microchemistry Laboratory for work on the protein microsequencing; P. Pedersen and the members of his lab for use of and assistance with the spectrometer; K.-W. Yau for helpful discussion; and C. L. Finch for assistance in preparing the manuscript. This work was supported by the Howard Hughes Medical Institute (R. L. H.) and the Medical Scientist Training Program (M. D. E.).

Received December 11, 1995; revised January 15, 1996.

References

Aderem, A. (1992). The MARCKS brothers: a family of protein kinase C substrates. Cell *71*, 713–716.

Bear, M.F. (1995). Mechanism for a sliding synaptic modification threshold. Neuron *15*, 1–4.

Blackstone, C.D., Moss, S.J., Martin, L.J., Levey, A.I., Price, D.L., and Huganir, R.L. (1992). Biochemical characterization and localization of a non-N-methyl-D-aspartate glutamate receptor subunit in rat brain. J. Neurochem. *58*, 1118–1126.

Bliss, T.V. P., and Collingridge, G.L. (1993). A synaptic model of memory: long-term potentiation in the hippocampus. Nature *361*, 31–39.

Chen, T.Y., and Yau, K.W. (1994). Direct modulation by Ca^{2+}-calmodulin of cyclic nucleotide-activated channel of rat olfactory receptor neurons. Nature *368*, 545–548.

Choi, D.W. (1995). Calcium: still center-stage in hypoxic-ischemic neuronal death. Trends Neurosci. *18*, 58–60.

Collingridge, G.L., and Lester, R.A.J. (1989). Excitatory amino acid receptors in the vertebrate central nervous system. Pharmacol. Rev. *41*, 143–210.

Constantine-Paton, M., Cline, H.T., and Debski, E. (1990). Patterned activity, synaptic convergence, and the NMDA receptor in developing visual pathways. Annu. Rev. Neurosci. *13*, 129–154.

Durand, G.M., Gregor, P., Zheng, X., Bennet, M.V. L., Uhl, G. R., and Zukin, R.S. (1992). Cloning of an apparent splice variant of the rat N-methyl-D-aspartate receptor NMDAR1 with altered sensitivity to polyamines and activators of protein kinase C. Proc. Natl. Aca. Sci. USA *89*, 9359–9363.

Ehlers, M.D., Tingley, W.G., and Huganir, R.L. (1995). Regulated subcellular distribution of the NR1 subunit of the NMDA receptor. Science *269*, 1734–1737.

Hollmann, M., Boulter, J., Maron, C., Beasley, L., Sullivan, J., Pecht, G., and Heinemann, S. (1993). Zinc potentiates agonist-induced currents at certain splice variants of the NMDA receptor. Neuron *10*, 943–954.

Hollmann, M., and Heinemann, S. (1994). Cloned glutamate receptors. Annu. Rev. Neurosci. *17*, 31–108.

James, P., Vorherr, T., and Carafoli, E. (1995). Calmodulin-binding domains: just two faced or multi-faceted? Trends Biochem. *20*, 38–42.

Kincaid, R.L., Vaughan, M., Osborne J.C., Jr., and Tkachuk, V.A. (1982). Ca^{2+}-dependent interaction of 5-dimethylaminonaphthalene-1-sulfonyl-calmodulin with cyclic nucleotide phosphodiesterase, calcineurin, and troponin I. J. Biol. Chem. *257*, 10638–10643.

Kutsuwada, T., Kashiwabuchi, N., Mori, H., Sakimura, K., Kushiya, E., Araki, K., Meguro, H., Masaki, H., Kumanishi, T., Arakawa, M., and Mishina, M. (1992). Molecular diversity of the NMDA receptor channel. Nature *358*, 36–41.

Lau, L.F., and Huganir, R.L. (1995). Differential tyrosine phosphorylation of N-methyl-D-aspartate receptor subunits. J. Biol. Chem. *270*, 20036–20041.

Laurie, D.J., and Seeburg, P.H. (1994). Regional and developmental heterogeneity in splicing of the rat brain NMDAR1 mRNA. J. Neurosci. *14*, 3180–3194.

Legendre, P., Rosenmund, C., and Westbrook, G.L. (1993). Inactivation of NMDA channels in cultured hippocampal neurons by intracellular calcium. J. Neurosci. *13*, 674–684.

Lieberman, D.N., and Mody, I. (1994). Regulation of NMDA channel function by endogenous Ca^{2+}-dependent phosphatase. Nature *369*, 235–239.

Liu, M., Chen, T.Y., Ahamed, B., Li, J., and Yau, K.W. (1994). Calcium-calmodulin modulation of the olfactory cyclic nucleotide–gated cation channel. Science *266*, 1348–1354.

MacDermott, A.B., Mayer, M.L., Westbrook, G.L., Smith, S.J., and Barker, J.L. (1986). NMDA-receptor activation increases cytoplasmic calcium concentration in cultured spinal cord neurons. Nature *321*, 519–522.

Mayer, M.L., Westbrook, G.L., and Guthrie, P.B. (1984). Voltage-dependent block by Mg^{2+} of NMDA responses in spinal cord neurons. Nature *309*, 261–263.

Mayer, M.L., and Westbrook, G.L. (1985). The action of N-methyl-D-aspartic acid on mouse spinal neurones in culture. J. Physiol. *361*, 65–90.

Medina, I., Filippova, N., Charton, G., Rougeole, S., Ben-Ari, Y., Khrestchatisky, M., and Bregestovski, P. (1995). Calcium-dependent inactivation of heteromeric NMDA receptor-channels expressed in human embryonic kidney cells. J. Physiol. *482*, 567–573.

Meguro, H., Mori, H., Araki, K., Kushiya, E., Kutsuwada, T., Yamazaki, M., Kumanishi, T., Arakawa, M., Sakimura, K., and Mishina, M. (1992). Functional characterization of a heteromeric NMDA receptor channel expressed from cloned cDNAs. Nature *357*, 70–74.

Monyer, H., Sprengel, R., Schoepfer, R., Herb, A., Higuchi, M., Lomeli, H., Burnashev, N., Sakmann, B., and Seeburg, P. (1992). Heteromeric NMDA receptors - molecular and functional distinction of subtypes. Science *256*, 1217–1221.

Moriyoshi, K., Masu, M., Ishii, T., Shigemoto, T., Mizuno, N., and Nakanishi, S. (1991). Molecular cloning and characterization of the rat NMDA receptor. Nature *354*, 31–37.

Petralia, R.S., Yokotani, N., and Wenthold, R.J. (1994). Light and electron microscope distribution of the NMDA receptor subunit NMDAR1 in the rat nervous system using a selective anti-peptide antibody. J. Neurosci. *14*, 667–696.

Phillips, W.D., Kopta, C., Blount, P., Gardner, P.D., Steinbach, J.H., and Merlie, J.P. (1991). ACh receptor-rich membrane domains organized in fibroblasts by recombinant 43-kilodalton protein. Science *251*, 568–570.

Roche, K.W., Tingley, W.G., and Huganir, R.L. (1994). Glutamate receptor phosphorylation and synaptic plasticity. Curr. Opin. Neurobiol. *4*, 383–388.

Rosenmund, C. and Westbrook, G.L. (1993a). Rundown of N-methyl-D-aspartate channels during whole-cell recording in rat hippocampal neurons: role of Ca^{2+} and ATP. J. Physiol. *470*, 705–729.

Rosenmund, C., and Westbrook, G.L. (1993b). Calcium-induced actin depolymerization reduces NMDA channel activity. Neuron *10*, 805–814.

Seeburg, P.H. (1993). The TINS/TiPS lecture: the molecular biology of glutamate receptor channels. Trends Neurosci. *16*, 359–365.

Sheng, M., Cummings, J., Roldan, L., Jan, Y., and Jan, L. (1994).

Changing subunit compostion of heteromeric NMDA receptors during development of rat cortex. Nature *368*, 144–147.

Sugihara, H., Moriyoshi, K., Ishii, T., Masu, M., and Nakanishi, S. (1992). Structures and properties of seven isoforms of the NMDA receptor generated by alternative splicing. Biochem. Biophys. Res. Commun. *185*, 826–832.

Tingley, W.G., Roche, K.W., Thompson, A.K., and Huganir, R.L. (1993). Regulation of NMDA receptor phosphorylation by alternative splicing of the C-terminal domain. Nature *364*, 70–73.

Tong, G., Shepard, D., and Jahr, C.E. (1995). Synaptic desensitization of NMDA receptors by calcineurin. Science *267*, 1510–1512.

Traynelis, S.F., Hartley, M., and Heinemann, S.F. (1995). Control of proton sensitivity of the NMDA receptor by RNA splicing and polyamines. Science *268*, 873–876.

Vyklicky, L. (1993). Calcium-mediated modulation of N-methyl-D-aspartate (NMDA) responses in cultured rat hippocampal neurones. J. Physiol. *470*, 575–600.

Wisden, W., and Seeburg, P.H. (1993). Mammalian ionotropic glutamate receptors. Curr. Opin. Neurobiol. *3*, 291–298.

Zorumski, C.F., Yang, J., and Fischbach, G.D. (1989). Calcium-dependent, slow desensitization distinguishes different types of glutamate receptors. Cell. Mol. Neurobiol. *9*, 95–104.